ISSN 1063-7710, Acoustical Physics, 2016, Vol. 62, No. 5, pp. 537–544. © Pleiades Publishing, Ltd., 2016.
Original Russian Text © V.I. Yusupov, A.N. Konovalov, V.A. Ul'yanov, V.N. Bagratashvili, 2016, published in Akusticheskii Zhurnal, 2016, Vol. 62, No. 5, pp. 531–539.

PHYSICAL ACOUSTICS

Generation of Acoustic Waves by CW Laser Radiation at the Tip of an Optical Fiber in Water

V. I. Yusupov[a,b,*], A. N. Konovalov[b], V. A. Ul'yanov[b], and V. N. Bagratashvili[b]

[a] *Il'ichev Pacific Institute of Oceanology, Far East Branch, Russian Academy of Sciences, ul. Baltiiskaya 43, Vladivostok, 690041 Russia*

[b] *Institute of the Problems of Laser and Information Technologies, Russian Academy of Sciences, ul. Pionerskaya 2, Troitsk, Moscow, 142190 Russia*

**e-mail: iouss@yandex.ru*

Received September 15, 2015

Abstract—We investigate the specific features of acoustic signals generated in water under the action of cw laser radiation with a power of 3 W at wavelengths of 0.97, 1.56, and 1.9 μm, emerging from an optical fiber. It is established that when a fiber tip without an absorbing coating is used, quasi-periodic pulse signals are generated according to the thermocavitation mechanism due to the formation and collapse of vapor–gas bubbles of millimeter size. In this case, the maximum energy of a broadband (up to 10 MHz) acoustic signal generated only at wavelengths of 1.56 and 1.9 μm is concentrated in the range of 4–20 kHz. It is shown that when there is no absorbing coating, an increase in the laser-radiation absorption coefficient in water leads to an increase in the frequency of generated acoustic pulses, while the maximum pressure amplitudes in them remain virtually constant. If there is an absorbing coating on the laser-fiber tip, a large number of small vapor–gas bubbles are generated at all laser-radiation wavelengths used. This leads to the appearance of a continuous amplitude-modulated acoustic signal, whose main energy is concentrated in the range of 8–15 kHz. It is shown that in this case, increasing the absorption coefficient of laser radiation in water leads to an increase in the power of an acoustic emission signal. The results can be used to explain the high therapeutic efficiency of moderate-power laser-fiber apparatus.

Keywords: cw laser radiation, acoustic pulses, optical fiber, moderate power

DOI: 10.1134/S1063771016050183

INTRODUCTION

It is well known that when optical radiation acts on a substance, perturbation of the medium occurs, which is accompanied by acoustic wave generation [1]. Optoacoustics is a field of science that systematizes scientific information on the effects of excitation of acoustic waves by optical radiation. One of the mechanisms for the optical generation of acoustic waves considered in optoacoustics is that external pulsed or modulated optical radiation absorbed in a medium, which can be gaseous, liquid, or solid, excites elastic perturbations in it due to thermal expansion. Optoacoustic effects are widely used because analysis of these perturbations allows reconstruction of various physical parameters of the studied medium [2–9]. Another method for exciting sound by optical radiation, which is applicable to liquids, e.g., water-containing media, including biological, is the generation of vapor–gas (VG) bubbles [10, 11]. For this, focused pulse laser radiation (LR) is used, which can create rather high energy density in the medium [11, 12]. At the instant a laser pulse arrives, due to intense heating caused by LR absorption and explosive boiling of the liquid, a VG bubble forms and rapidly increases in size in the beam-focusing region. When it reaches its maximum radius, it rapidly collapses. In this case, the recorded acoustic signal consists of a series of short pulses followed by decaying oscillations. The first pulse corresponds to the arrival of a shock wave from fast laser heating and explosive water boiling, and the second and subsequent pulses correspond to the arrival of shock waves from cavitation collapse of the formed VG bubble [1]. With a further increase in the laser pulse energy density, more complex sound generation processes develop, which are associated with optical breakdown [1].

Sound can also be generated under the action of cw LR on a substance. This mechanism of optical acoustic wave generation in a liquid was first considered in [13] and called thermocavitation. It involves the formation of an overheated region at the focal spot of focused LR, after which fluctuations initiate explosive boiling of the liquid with the formation of a rapidly expanding VG bubble [13, 14]. During this thermo-

cavitation, plasma is not produced because of the rather low LR intensity. In contrast to a plasma, whose temperature can reach 10 000°, the heating temperature of, e.g., water during thermocavitation, which is determined by the spinodal, is ~300°C. The recorded acoustic signal in a single thermocavitation event is the same as in the case of bubbles generated by pulse LR and consists of a series of short pulses followed by decaying oscillations. As shown in [13], thermocavitation is not a single, but a quasi-periodic process. In this case, the periodicity and amplitudes of shock waves strongly depend on the distance from the cell wall to the focal point of cw laser radiation in the liquid: when radiation is focused on the wall, the frequency is maximized and the pulse amplitude is minimized.

In the last decade, moderate-power laser apparatus (1–10 W) with a fiber output [15–17] have been widely used in experimental studies and practical applications, including medicine. It has been shown in a number of studies [18–21] that in water and water-saturated tissues, active hydrodynamic processes develop near the working laser-fiber tip under the action of cw LR. These processes are accompanied by the formation and collapse of VG bubbles, the appearance of bubble microjets, circulating liquid flows, and acoustic signals generated in a wide frequency range from fractions of a hertz to ten or more megahertz. The characteristics of these processes and acoustic emission (AE) signals determined by them must substantially depend on the LR absorption coefficient and the presence of an absorbing coating at the laser-fiber tip [18–21], which actually transforms the tip into a "point" heat source. Knowledge of the generation mechanism and specific features that arise during continuous laser-induced acoustic vibrations is also necessary to understand the mechanism of the high therapeutic efficiency of moderate-power laser apparatus [16, 17, 21]. In several studies, it was shown that acoustic signals generated near the laser-fiber tip in a biological tissue as a result of laser-induced hydrodynamic processes make a significant contribution to the mechanism of the therapeutic effect of moderate-power LR [22, 23].

The objective of this study was to investigate the features of acoustic signals generated in water under the action of cw moderate-power LR, which emerges from an optical fiber, for substantially different optical absorption coefficients.

EXPERIMENTAL

Moderate-power LS-0.97-IRE-Polyus lasers with a wavelength of 0.97 μm (with a power of up to 10 W), LS-1.56-IRE-Polyus lasers with a wavelength of 1.56 μm (up to 5 W), and LS-1.9-IRE-Polyus lasers with a wavelength of 1.9 μm (up to 3 W) with a 400-μm-diameter quartz fiber were used as LR sources. Radiation at the aforementioned wavelengths was generated by semiconductor laser diodes (0.97 μm) and erbium- (1.56 μm) and thulium-activated (1.94 μm) fibers. In all experiments, the laser power at the fiber output was 3 W, and the short-term power deviations from the mean value were within 4%. For the chosen LR wavelengths, the absorption coefficients in water differ substantially. Their values are 0.47 cm^{-1} for 0.97 μm, 10 cm^{-1} for 1.56 μm, and 92 cm^{-1} for 1.9 μm [24]. Two main laser-action regimes were used in the investigations: (1) a fiber tip without an absorbing coating and (2) a fiber tip with an absorbing coating. The absorbing coating was applied to the working tip of the quartz fiber via its short-duration (about 1 s) contact with a wooden bar at a laser power of ~3 W, which resulted in stable coating of the fiber tip with a layer of amorphous carbon [19–21].

To record broadband acoustic signals, the working tip of the laser fiber was placed in a water-filled vessel with dimensions of 24 x 40 x 24 cm. At a distance of ~1 cm from the fiber tip, an 8103 broadband hydrophone (B&K, Denmark) with a band of 0.1 Hz–80 kHz (the sensitivity is 211 dB rel. 1 V/μPa) and a needle hydrophone (Precision Acoustics, UK) with a diameter of 1 mm with a preamplifier (its bandwidth is 10 kHz–50 MHz and the sensitivity is 241 dB rel. 1 V/μPa). Acoustic signals from the hydrophones were recorded using a GDS 72304 (GW Instek, Taiwan) four-channel digital storage oscilloscope with a passband of 300 MHz. The AE signal energy was estimated under the assumption of a spherical acoustic wave [25]:

$$E = \frac{4\pi r^2}{\rho c}\int p^2 dt, \qquad (1)$$

where r is the distance from the emission center to the hydrophone, ρ is the water density, c is the velocity of sound in water, p is the pressure amplitude, and t is the time.

Laser-induced hydrodynamic processes that occur near the fiber tip in water were optically recorded by a Fastcam SA-3 (Photron, Japan) high-speed camera at a speed of 10000 fps. To monitor the spectral composition and power of optical radiations, we used a USB4000 (Ocean Optics, United States) fiber-optic spectrum analyzer (combined with a PC) with a resolution of ~1.5 nm and an operating range of 200–1100 nm. We also used a FieldMaster power meter with an LM-10HTD measuring head (Coherent, United States).

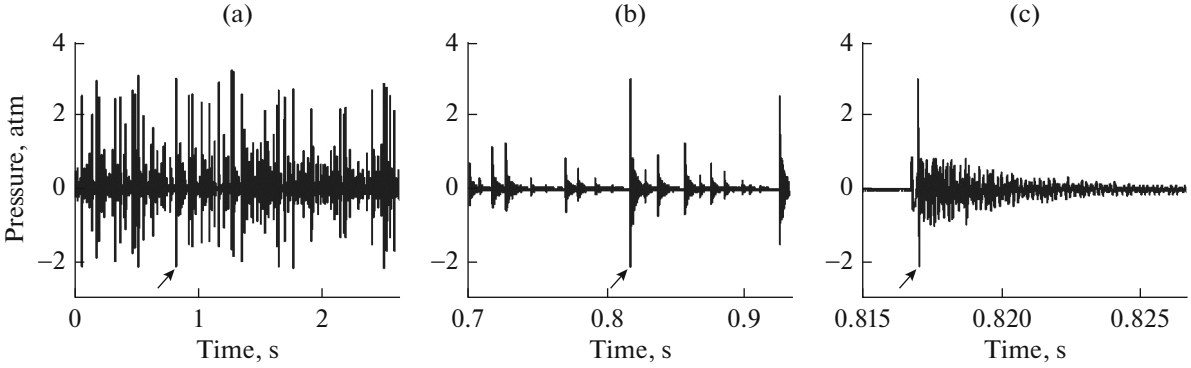

Fig. 1. Fragments of acoustic signal recorded with 8103 broadband hydrophone for fiber tip without coating at laser wavelength of 1.9 μm on different time scales. Pressure is recalculated for distance of 1 mm. The arrow indicates a pressure pulse present on all three scales.

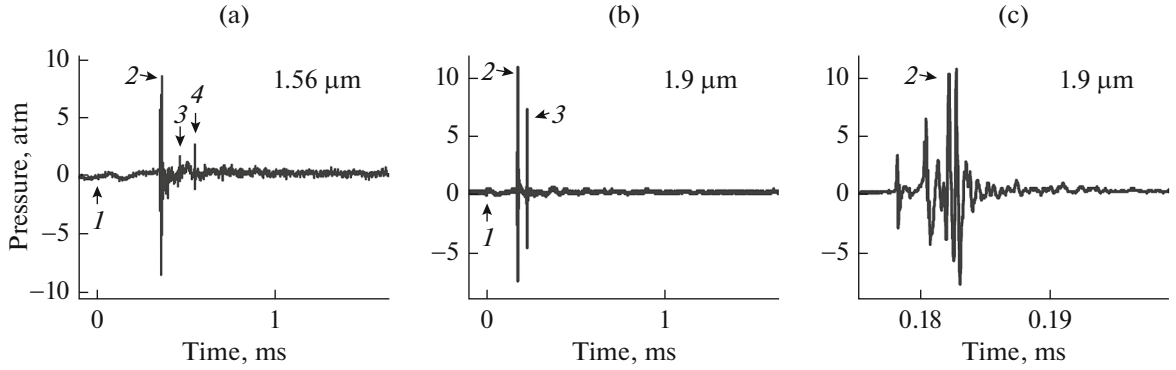

Fig. 2. Fragments of acoustic signals recorded with needle hydrophone for fiber tip without coating for laser wavelengths of 1.56 and 1.9 μm on different time scales. Pressure is recalculated for distance of 1 mm. Arrows show (*1*) onset of precursor, (*2*) most intense pressure pulse, and (*3*, *4*) subsequent pressure pulses.

RESULTS AND DISCUSSION

For a fiber tip without a coating that was immersed in water, AE signals were recorded at a cw LR power of 3 W only at wavelengths of 1.56 and 1.9 μm. Figure 1 shows fragments of an acoustic signal recorded by the broadband hydrophone on different time scales for a laser wavelength of 1.9 μm. One can see that in this case, quasi-periodic (with a frequency in the range of 60–100 pulses/s) pulse signals are generated near the laser-fiber tip. The maximum pressure amplitudes in them reach 3 atm. Each such pulse signal is characterized by a bipolar "precursor" with a quite high amplitude, which is followed by a high-power bipolar pressure pulse with subsequent decaying oscillations (Fig. 1c). Figure 2 presents the case where the period between the precursor and the high-power pulse was ~0.2 ms and the decaying oscillations lasted more than 10 ms. Analysis of the recorded signals showed that both the precursor and the high-power pulse always began with a pressure increase. In this case, the amplitude of the positive pressure in the precursor was always 15–25% of the amplitude of the next high-power pulse, and the period between these pulses decreased on average with a decrease in the pressure-pulse amplitude. As for the AE signal recorded by the broadband hydrophone at a laser wavelength of 1.56 μm, it is also a quasi-periodic sequence of pulse signals whose shape hardly differs at all from that of the above-described pulses for a wavelength of 1.9 μm. Note that the pulse amplitudes lie within the same ranges and the main difference is that in comparison to a wavelength of 1.9 μm, pulses are generated much more seldom, with a frequency of 5–15 pulses/s.

The initial complex shape of acoustic signals produced near the fiber tip under the laser action can be examined in more detail using signals recorded with the needle hydrophone. Figure 2 shows typical fragments of pulse acoustic signals for laser wavelengths of 1.56 and 1.9 μm. It is seen that for both wavelengths, the shapes of pressure pulses resemble each other. A bipolar precursor is initially recorded, after which several high-power (the amplitudes at a distance of 1 mm

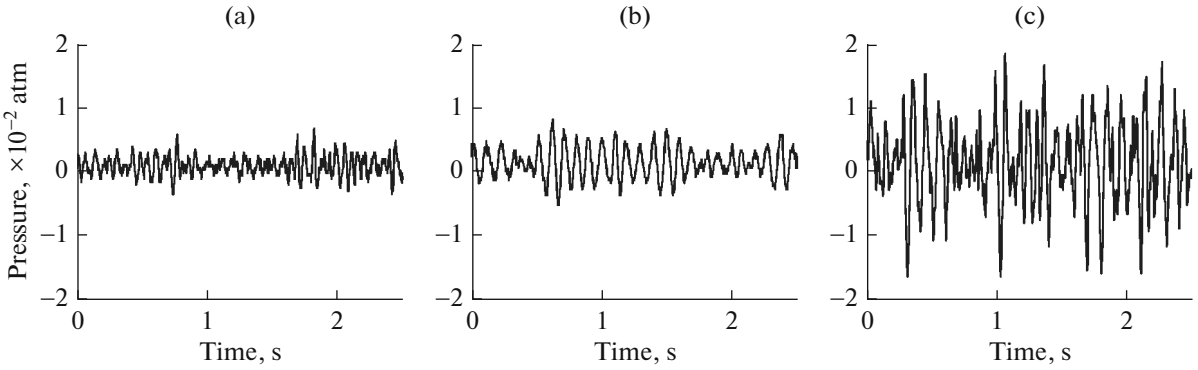

Fig. 3. Fragments of acoustic signals recorded with 8103 broadband hydrophone for fiber tip with absorbing coating at laser wavelengths of (a) 0.97, (b) 1.56, and (c) 1.9 μm. Pressure is recalculated for distance of 1 mm.

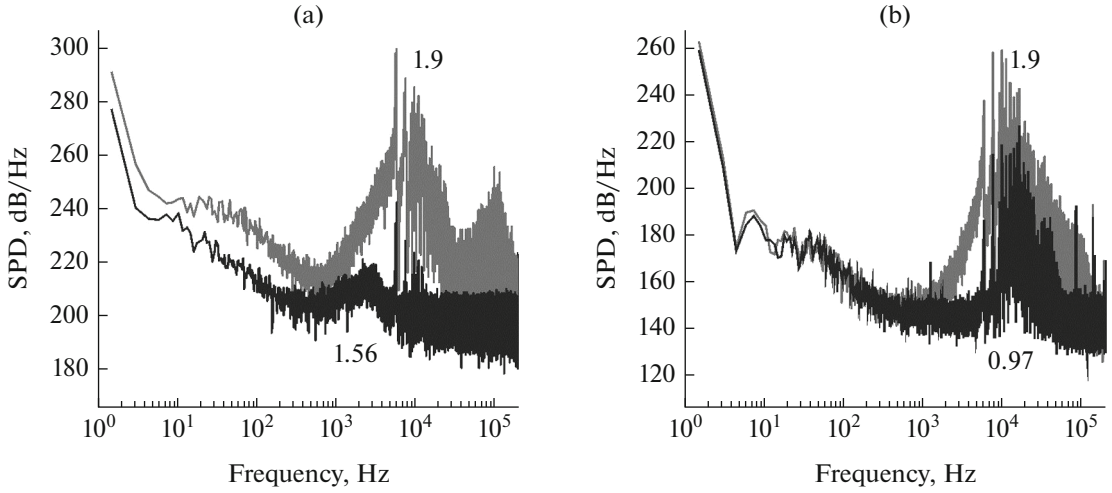

Fig. 4. Spectral power densities of acoustic signals that were recorded with the 8103 broadband hydrophone for the fiber tip (a) without and (b) with an absorbing coating at different laser wavelengths (in microns). The pressure is recalculated for a distance of 1 mm.

are ~10 atm) bipolar pressure pulses follow with subsequent decaying oscillations. The time intervals between the onset of precursor *1* and the first (most powerful) pulse *2* (Figs. 2a, 2b) were as follows: ~0.36 ms for a wavelength of 1.56 μm and ~0.2 ms for 1.9 μm. After the first powerful pulse *2* (Figs. 2a, 2b) at a wavelength of 1.56 μm, two pulses follow (*3* and *4* in Fig. 2a), while at a wavelength of 1.9 μm, there is one pulse (*3* in Fig. 2b). A more detailed examination (Fig. 2c) shows that the high-power pulse (*2* in Fig. 2b) splits into a series of short bipolar pulses in an interval of ~10 μs (their FWHM range from 0.06 to 0.2 μs).

In the case of the fiber tip with an absorbing coating, AE signals were recorded at all experimentally used wavelengths. Figure 3 shows some typical fragments of acoustic signals recorded with the broadband hydrophone. It is seen that if there is an absorbing coating at the laser-fiber tip, a continuous amplitude-modulated acoustic signal is generated for all used wavelengths. In this case, the characteristic frequencies of

Power of acoustic signal generated in water near fiber tip without and with absorbing coating and recorded with 8103 broadband hydrophone at different wavelengths of laser radiation with power of 3 W

Wavelength, μm		0.97	1.56	1.9
Acoustic signal power, μW	Without coating	0	8.8 ± 1.2	830 ± 43
	With coating	0.3 ± 0.1	0.7 ± 0.2	6.3 ± 1.1

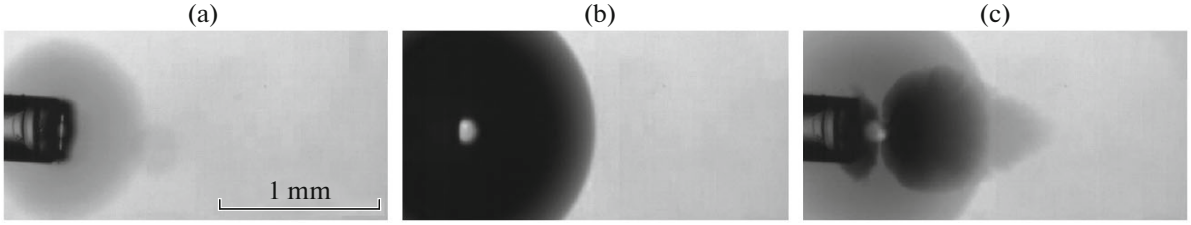

Fig. 5. Fragment of consecutive frames of high-speed film during generation of VG bubble near fiber tip without coating under action of cw laser radiation with wavelength of 1.9 μm and power of 3 W. The period between individual frames is 100 μs.

these signals differ slightly (their range is 8–15 kHz), and the average signal amplitude gradually builds up with an increase in the laser wavelength.

Figure 4 shows the characteristic spectra of signals recorded with the 8103 broadband hydrophone for fiber tips with and without an absorbing coating for different laser wavelengths. For the case with an absorbing coating (Fig. 4b), in order not to clutter the figure, only the spectra at wavelengths of 0.97 and 1.9 μm are shown, because the spectrum at 1.56 μm has the same characteristic features as those for the other laser wavelengths and is positioned between these curves. All the spectra shown in Fig. 4 have many common features: in the low-frequency region (<400 Hz), the spectral power density (SPD) on average decreases, while in the "high-frequency" region (10^3–3×10^4 Hz), the SPD first on average increases and then decreases. In this case, alternate narrow local maxima that, according to estimates, are associated with the acoustic resonances of the water-filled vessel are observed in the high-frequency region. For the fiber tip without a coating (Fig. 4a), the maximum SPD values in this region correspond to one of such local maxima at a frequency of ~6 kHz for both wavelengths. For the fiber tip with an absorbing coating (Fig. 4b), the maximum SPD values are observed at a frequency of ~15 kHz for a wavelength of 0.97 μm and at ~10 kHz for 1.56 and 1.9 μm. Comparison of the acoustic spectra without a coating (Fig. 4a) with the analogous spectra for the absorbing coating (Fig. 4b) shows that application of an absorbing coating to the laser-fiber tip 1.56 and 1.9 μm leads to a substantial decrease in the SPD level of the acoustic signal in the entire frequency range considered and to shifts of the local maxima toward higher frequencies for laser wavelengths of 1.56 and 1.9 μm.

The table presents the averaged power values of acoustic signals generated in water and recorded with the 8103 broadband hydrophone at a laser power of 3 W. As follows from this table, in both cases (without and with an absorbing coating), the minimum values of the AE signal power correspond to a wavelength of 0.97 μm, and as the laser wavelength increases, the acoustic signal power gradually increases and reaches a maximum at a laser wavelength of 1.9 μm.

The optical recording with a high-speed Fastcam SA-3 camera showed that when there is no coating on the laser-fiber tip and wavelengths of 1.56 and 1.9 μm are used, quasi-periodic generation of large (up to 1–3 mm in diameter) VG bubbles is observed (Fig. 5). As one can see in Fig. 5, the bubble that formed near the fiber tip reached its maximum size of ~1.7 mm within a time of 100 μs, then collapsed within approximately the same time via the cavitation process, and it is as though it again expanded to ~0.7 mm with simultaneous displacement toward the free liquid (from the fiber tip).

The bubble generation pattern abruptly changes if an absorbing coating is deposited on the laser-fiber tip (Fig. 6). In this case, a large number of small (up to 60 μm in diameter) VG bubbles are generated near the tip and move from the fiber tip toward the free liquid at a velocity of ~100 mm/s. A similar qualitative pattern is observed for all used laser wavelengths; as the laser wavelength increases, a slight gradual increase in the average size of VG bubbles is observed: from 18 ±

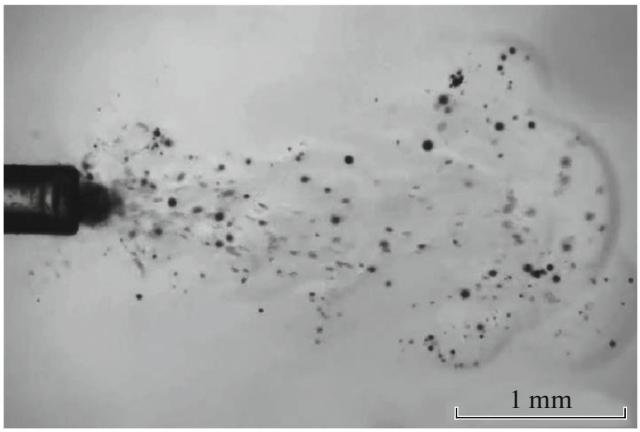

Fig. 6. Frame of high-speed film during generation of VG bubbles near fiber tip with absorbing coating under action of cw laser radiation with wavelength of 1.9 μm and power of 3 W.

9 μm (for a wavelength of 0.97 μm) to 25 ± 13 μm (1.56 μm) and to 38 ± 19 μm (1.9 μm).

Let us consider the possible mechanisms of generation of acoustic vibrations that allow explanation of the obtained effects. When the laser-fiber tip has no coating, sound is generated under the action of cw laser radiation according to the thermocavitation mechanism [13]. Near the laser fiber in water, an overheated region is initially formed owing to the LR absorption; subsequently, owing to fluctuations, explosive boiling of the liquid occurs with the formation of a rapidly expanding VG bubble. After the bubble reaches its maximum size, it also rapidly collapses (Fig. 5) and may then again expand (but in this case, its maximum size is smaller) and collapse several times. In the recorded acoustic signal, as is seen in Figs. 2a and 2b, the precursor, which is the first bipolar pulse *1*, is associated with explosive water boiling, after which a VG bubble is formed, expands (a positive pressure), and shrinks (a negative pressure). The second, the most powerful pulse (*2* in Figs. 2a, 2b) and the subsequent pressure pulses (*3* and 4 in Fig. 2a and *3* in Fig. 2b) are determined by the cavitation collapse of the formed VG bubble [1]. The bubble collapse time and its maximum radius R_{max} are interrelated via the linear dependence [26]

$$T_c = 0.915R_{max}\sqrt{\frac{\rho}{p_0 - p_v}}, \quad (2)$$

where ρ is water density, p_0 is the external pressure (~100 kPa), and p_v is the saturated-vapor pressure (2.33 kPa at 20°C). For a bubble with the maximum radius $R_{max} = 0.85$ mm, like in Fig. 5, under these conditions, $T_c \approx 78$ μs according to (2); consequently, the total duration of the precursor from the moment of the onset of explosive-boiling to bubble collapse with the generation of a high-power pressure pulse is ~156 μs. The potential energy of the formed bubble E is determined by its maximum radius R_{max} and the difference between the hydrostatic pressure p_0 and the vapor pressure inside the bubble p_v [27]:

$$E = \frac{4\pi}{3}(p_0 - p_v)R_{max}^3. \quad (3)$$

For a bubble with the maximum radius $R_{max} = 0.85$ mm (as in Fig. 5), according to (3), $E \approx 0.25$ mJ, and the potential energy of bubbles with a maximum radius of ~1.5 mm observed experimentally is ~1.3 mJ. When a bubble is compressed to a very small size, the potential energy (3) is converted into the kinetic energy of a high-speed (~10^3 m/s [28]) cumulative jet and into the acoustic energy of a shock wave propagating in all directions [29]. When a bubble collapses near the solid wall of the laser-fiber tip, this jet is directed toward the wall [28]. It is known that such cumulative jets can damage the surface of a quartz-fiber tip, forming micron-sized holes, cracks, and other flaws on it [20].

It is obvious that the thermocavitation efficiency must significantly depend on the LR absorption coefficient in water, and this is shown experimentally. For a wavelength of 0.97 μm, its value (0.47 cm^{-1}) for the used laser power of 3 W is insufficient for rapid heating of the liquid and excitation of explosive boiling; therefore, when the fiber tip without a coating is used, acoustic waves are not generated (see table). Increasing the absorption coefficient to 10 cm^{-1} (the wavelength is 1.56 μm) leads to the generation of acoustic waves according to the thermocavitation mechanism and generation of high-power pulses at a repetition rate of 5–15 pulses/s. A further increase in the absorption coefficient to 92 cm^{-1} (1.9 μm) does not lead to an increase in the maximum pressure values in pulses but significantly increases their generation frequency to 60–100 pulses/s.

The train of damped oscillations recorded after the first high-power pulse (*2* in Fig. 2) is associated with the fact that after the first collapse, a cavitation bubble pulsates at a frequency close to its natural oscillation frequency. If the surface tension for free water is disregarded, the bubble pulsation frequency is [30]

$$F \approx \frac{1}{2\pi R}\left(\frac{3\gamma p_0}{\rho}\right)^{1/2}, \quad (4)$$

where γ is the ratio of the specific heat for the bubble gas, ρ is the water density, and p_0 is the hydrostatic pressure. Taking into account that the period between pulses *2* and *3* (Fig. 2a) is ~0.1 ms (F ~ 10 kHz), assuming that $\gamma = 1.4$, $\rho = 10^3$ kg/m^3, and $p_0 \approx 100$ kPa, and using (4), we obtain $R \approx 340$ μm for the radius of a resonance bubble.

After an absorbing coating is applied to the fiber tip, a portion of the laser energy (~30%) is absorbed in a carbon layer and heats it. If the fiber tip is in air and the LR power reaches 3 W, in addition to the principal lasing line, broadband radiation in the visible and near-IR spectrum regions emerges from the fiber tip, which is responsible for tip heating to high temperatures (~500–700°C). If such a fiber tip is in water, its cooling is more intense and this broadband radiation is absent, thus indicating that the tip surface has lower temperatures. However, the fiber-tip heating is still sufficient for the formation of VG bubbles as a result of explosive boiling in water near its surface [19, 21]. Therefore, in the presence of an absorbing coating on the fiber tip, an acoustic signal is generated even at a wavelength of 0.97 μm (see table). An increase in the power of the acoustic signal recorded with the 8103 broadband hydrophone with an increase in the laser wavelength (see the table) can be explained by the fact

that a significant portion of the laser energy (~70%) passes through the absorbing coating on the fiber tip and is absorbed in the liquid. As a result, the liquid near the fiber tip is heated to a higher degree, as the radiation absorption coefficient in water increases. As is known from [24], it increases considerably with an increase in the wavelength from 0.97 (0.47 cm^{-1}) to 1.56 (10 cm^{-1}) and to 1.9 μm (92 cm^{-1}). Therefore, as the laser wavelength increases, the efficiency of formation of VG bubbles increases as well, and the AE-signal power simultaneously increases.

CONCLUSIONS

The specific features of acoustic signals generated in water under the action of cw laser radiation with a power of 3 W and wavelengths of 0.97, 1.56, and 1.9 μm, which emerges from an optical fiber, were investigated at substantially different optical absorption coefficients in water: 0.47, 10, and 92 cm^{-1}, respectively.

It was established that for the fiber tip without an absorbing coating, which is immersed in water, AE signals are detected only at wavelengths of 1.56 and 1.9 μm. In this case, millimeter-size VG bubbles quasi-periodically form and collapse near the laser-fiber tip as a result of the formation of an overheated region due to explosive boiling of the liquid. Thus, the observed generation of quasi-periodic pulse signals occurs according to the thermocavitation mechanism [13]; in this case, the maximum energy of a broadband (up to 10 MHz) acoustic signal is concentrated within a range of 4–20 kHz with a local maximum at a frequency of ~6 kHz. It is shown that in this case, an increase in the LR absorption coefficient in water leads only to an increase in the frequency of formation of VG bubbles for operating wavelengths of 1.56 and 1.9 μm, while the maximum dimensions of the produced bubbles do not change reliably. In this case, the generation frequency of acoustic pulses correspondingly increases, and the acoustic power considerably increases as well (from 8.8 ± 1.2 μW to 830 ± 43 μW).

The pattern changes appreciably in the presence of an absorbing coating on the laser-fiber tip. In this case, due to the partial (~30% of the total power regardless of the wavelength) absorption of LR, the laser-fiber tip is heated. This leads to the generation of a large number of small (up to 60 μm) VG bubbles near the fiber tip, which move from the tip toward the free liquid. This process is accompanied by the appearance of a continuous amplitude-modulated acoustic signal, whose main energy is concentrated in a range of 8–15 kHz. It is shown that in the case of an absorbing coating for the used laser wavelengths (0.97, 1.56, and 1.9 μm), an increase in the LR absorption coefficient in water leads to a slight reliable increase in the size of the formed VG bubbles, which is caused by an increase in their production efficiency. As a result, the generated acoustic signal power correspondingly increases from 0.3 ± 0.1 to 6.3 ± 1.1 μW.

Moderate-power laser apparatus with wavelengths of 0.97, 1.56, and 1.9 μm and a fiber output [15] are widely used not only in experimental physics [18–21] but also in experimental biology [22, 23] and medicine [16, 17, 21]. Results that refine the generation mechanism and describe the characteristic features of acoustic vibrations that arise in water under the action of cw fiber laser radiation can be used in various areas, including explanation of the high therapeutic efficiency of moderate-power laser apparatus [16, 17, 21, 31, 32].

ACKNOWLEDGMENTS

This study was supported by the Russian Science Foundation, project no. 14-25-00055.

REFERENCES

1. L. M. Lyamshev, Phys.-Usp. **30**, 252–279 (1987).
2. S. V. Egerev, L. M. Lyamshev, and O. V. Puchenkov, Phys.-Usp. **33** 739 (1990).
3. Kel'bert, M.Ya. and Sazonov, I.A., *Propagation of Pulses in Liquids* (Mauka, Moscow, 1991) [in Russian].
4. S. V. Egerev and A. A. Pashin, Acoust. Phys. **39**, 43 (1993).
5. V. B. Oshurko, Quant. Electr. **35**, 185 (2005).
6. K. Maslov and L. V. Wang, J. Biomed. Optics **13**, 024006 (2008).
7. A. A. Karabutov, N. B. Podymova, and V. S. Letokhov, Appl. Phys. B **63**, 545 (1996).
8. M. L. Lyamshev, Acoust. Phys. **44**, 608(1998).
9. A. V. Fokin, Akust. Zh. **41**, 314 (1995).
10. W. D. Song, M. H. Hong, B. Lukyanchuk, and T. C. Chong, J. Appl. Phys. **95**, 2952 (2004).
11. A. Vogel and W. Lauterborn, J. Acoust. Soc. Am. **84**, 719 (1988).
12. A. Philipp and W. Lauterborn, J. Fluid Mech. **361**, 75 (1998).
13. S. F. Rastopov and A. T. Sukhodolsky, Proc. SPIE—Int. Soc. Opt. Eng. **1440**, 127 (1991).
14. J. P. Padilla-Martinez, C. Berrospe-Rodriguez, and G. Aguilar, Phys. Fluids **26**, 122007 (2014).
15. V. P. Gapontsev, V. P. Minaev, V. I. Savin, and I. E. Samartsev, Quant. Electr. **32**, 1003 (2002).
16. B. I. Sandler, L. N. Sulyandziga, V. M. Chudnovskii, V. I. Yusupov, O. V. Kosareva, and V. S. Timoshenko, *Prospects of Cure of Histogenic Compression Forms of Lumbosacral Radiculitises with the Help of Puncture Nonendoscopic Laser Operations* (Dal'nauka, Vladivostok, 2004) [in Russian].

17. V. A. Privalov, I. V. Krochek, I. A. Abushkin, I. I. Shumilin, A. and V. Lappa, Vestn. Eksper. Klin. Khirur. **2**, 19 (2009).
18. V. I. Yusupov, V. V. Bulanov, V. M. Chudnovskii, and V. N. Bagratashvili, Laser Phys. **24**, 5601 (2014).
19. V. I. Yusupov, V. M. Chudnovskii, and V. N. Bagratashvili, Laser Phys. **20**, 1641 (2010).
20. V. I. Yusupov, V. M. Chudnovskii, and V. N. Bagratashvili, Laser Phys. **21**, 1230 (2011).
21. V. I. Yusupov, V. M. Chudnovskii, and V. N. Bagratashvili, in *Hydrodynamics – Advanced Topics*, Ed. by H. E. Schulz, A. L. A. Simoes, and R. J. Lobosco, (InTech, Croatia, 2011), pp. 95–118. DOI: doi 10.13140/2.1.4838.9122
22. R. K. Chailakhyan, V. I. Yusupov, Yu. F. Gorskaya, A. I. Kuralesova, Yu. V. Gerasimov, A. P. Sviridov, A. Kh. Tambiev, N. N. Vorob'eva, A. G. Grosheva, V. V. Shishkova, I. L. Moskvina, and V. N. Bagratashvili, Byull. Eksper. Biol. Medits. **158**, 640 (2014).
23. R. K. Chailakhyan, V. I. Yusupov, A. P. Sviridov, Yu. V. Gerasimov, A. Kh. Tambiev, N. N. Vorob'eva, A. I. Kuralesova, I. L. Moskvina, V. N. Bagratashvili, Biomed. Radioelektr., No. 2, 36 (2013).
24. R. Deng, Y. He, Y. Qin, Q. Chen, L. Chen, and Y. Xuebao, J. Remote Sensing **16**, 192 (2012).
25. R. H. Cole, *Underwater Explosions* (Princeton Univ., Princeton, 1948).
26. J. B. Keller and M. Miksis, J. Acoust. Soc. Am. **68**, 628 (1980).
27. C. E. Brennen, *Cavitation and Bubble Dynamics* (Oxford Univ., Oxford, 1995).
28. A. Vogel, W. Lauterborn, and R. Timm, J. Fluid Mech. **206**, 299 (1989).
29. A. Vogel and V. Venugopalan, Chem. Rev. **103**, 577 (2003).
30. M. Minnaert, Philos. Mag. **16**, 235 (1933).
31. A. L. Sokolov, K. V. Lyadov, M. M. Lutsenko, S. V. Lavrenko, A. A. Lyubimova, G. O. Verbitskaya, V. P. Minaev, Angiol. Sosud. Khirurg. **15**, 69 (2009).
32. N. E. Chernekhovskaya, A. V. Geinits, O. V. Lovacheva, and A. V. Povalyaev, *Lasers in Endoscopy* (MEDpress, Moscow, 2011) [in Russian].

Translated by A. Seferov